

## Spatiotemporal expression of AP-2/myosin $\text{VI}$ in mouse cochlear IHCs and correlation with auditory function

Xiang Gu & Ling Lin

To cite this article: Xiang Gu & Ling Lin (25 Apr 2024): Spatiotemporal expression of AP-2/myosin  $\text{VI}$  in mouse cochlear IHCs and correlation with auditory function, Acta Oto-Laryngologica, DOI: [10.1080/00016489.2024.2341126](https://doi.org/10.1080/00016489.2024.2341126)

To link to this article: <https://doi.org/10.1080/00016489.2024.2341126>



© 2024 The Author(s). Published by Informa UK Limited, trading as Taylor & Francis Group



Published online: 25 Apr 2024.



Submit your article to this journal [↗](#)



Article views: 210



View related articles [↗](#)



View Crossmark data [↗](#)

# Spatiotemporal expression of AP-2/myosin VI in mouse cochlear IHCs and correlation with auditory function

Xiang Gu and Ling Lin

Department of Otolaryngology Head and Neck Surgery, The Central Hospital of Wuhan, Tongji Medical College, Huazhong University of Science and Technology, Wuhan, China

## ABSTRACT

**Background:** Recycling of synaptic vesicles plays an important role in vesicle pool replenishment, neurotransmitter release and synaptic plasticity. Clathrin-mediated endocytosis (CME) is considered to be the main mechanism for synaptic vesicle replenishment. AP-2 (adaptor-related protein complex 2) and myosin VI are known as key proteins that regulate the structure and dynamics of CME.

**Objective:** This study aims to reveal the spatiotemporal expression of AP-2/myosin VI in inner hair cells (IHCs) of the mouse cochlea and its correlation with auditory function.

**Material and Methods:** Immunofluorescence was used to detect the localization and expression of AP-2 and myosin VI in cochlear hair cells (HCs) of CBA/CaJ mice of various ages. qRT-PCR was used to verify the differential expression of AP-2 and myosin VI mRNA in the mouse cochlea, and ABR tests were administered to mice of various ages. A preliminary analysis of the correlation between AP-2/myosin VI levels and auditory function was conducted.

**Results:** AP-2 was located in the cytoplasmic region of IHCs and was mainly expressed in the basal region of IHCs and the area near ribbon synapses, while myosin VI was expressed in the cytoplasmic region of IHCs and OHCs. Furthermore, AP-2 and myosin VI were not significant detected in the cochleae of P7 mice; the expression level reached a peak at P35 and then decreased significantly with age. The expression patterns and expression levels of AP-2 and myosin VI in the cochleae of the mice were consistent with the development of the auditory system.

**Conclusions and Significance:** AP-2 and myosin VI protein expression may differ in mice of different ages, and this variation probably leads to a difference in the efficiency in CME; it may also cause a defect in IHC function.

## ARTICLE HISTORY

Received 19 February 2024

Revised 1 April 2024

Accepted 4 April 2024

## KEYWORDS

Inner hair cells; hearing; aging; AP-2; myosin VI

Hair cells (HCs) in the cochlea play a critical role in converting sound waves into neural signals for hearing [1]. Previous studies using mouse models showed that acoustic injury of the auditory system is caused by multiple factors and that most of the hearing loss induced by noise, ototoxic drugs, inflammation and aging is caused by damage to HCs [2–4]. The ribbon synapse, an important structure between inner HCs (IHCs) and spiral ganglion neurons (SGN), is the primary synaptic structure in the sound conduction pathway and plays a critical role in sound signal transmission [5]. The maintenance of hearing depends on the release of neurotransmitters from ribbon synapses of cochlear IHCs onto auditory afferent fibers and on intact mechanical–electrical transduction [2]. Synaptic pathology of IHCs is one of the main causes of sensorineural hearing loss (SNHL) [6]. Regulation of synaptic vesicle number and maintenance of neurotransmitter release depends on endocytosis, while vesicle replenishment is a crucial process that occurs during vesicle turnover in the presynaptic membrane [7,8]. Clathrin-mediated endocytosis (CME) is thought to be the main mechanism for synaptic vesicle replenishment after neurotransmitter release [9], AP-2 acts as a key protein in

this endocytic process by binding to different proteins and other molecules [10,11]. Myosin VI is one of the molecules that can provide energy for vesicle replenishment by decomposing ATP [12,13]. AP-2 collects myosin VI to mediate endocytic vesicle fission [14], a process that is of great significance for CME. Although both AP-2 and myosin VI have been extensively studied in the central nervous system, they have not been well studied in the peripheral nervous system, particularly in auditory cochlear HCs.

CBA/CaJ mice are an excellent mouse strain in which to study auditory development. Their cochlear maturation and auditory function are established after birth [15,16], while the synaptic connections between IHCs and SGNs are established before birth. In the postnatal period, a large number of synaptic structures require further precise construction and modification [17]. Thus, HC synapses may be the initial target of age-related hearing loss (ARHL). Changes in synapse number, structure and function may be closely related to hearing dysfunction [18]. Previous studies have found that onset of hearing in mice occurs 10–12 days after birth [15]. We used CBA/CaJ mice of different ages to analyze whether the first and last stages of hearing formation and

dysfunction are related to AP-2/myosin VI, two potential key molecules in the regulation of endocytosis. Study of the localization and expression of these two proteins at different ages is critical for exploring the molecular mechanisms of IHC endocytosis and the synaptic pathology of ARHL.

## Materials and methods

### Animals

In this study, CBA/CaJ mice with normal Preyer's reflex were provided by the Experimental Animal Center of the Tongji Medical College, Huazhong University of Science and Technology. P7, P15, P35, 16-month-old and 8-week-old male mice were randomly selected and divided into 5 groups according to age, with 20 animals in each group (40 ears). All procedures were conducted in accordance with the guide for the care and use of laboratory animals approved by the Laboratory Animal Welfare and Ethics Committee of the Central Hospital of Wuhan.

### Auditory-evoked brainstem response (ABR) analysis

The Nicolet Compass system was used to alternately stimulate the two ears with clicks at a rate of 23.1 times per second. The bandpass filter was 100–3000 Hz, the analysis time was 10 ms, and the number of overlays was 1024. The acoustic stimulation intensity started at 80 dB SPL. It was first decreased by 10 dB at a time and then decreased by 5 dB at a time. The response thresholds to 4-, 8-, 16- and 32-kHz tone bursts were recorded. This process was repeated two times.

### Preparation of the organ of corti

Under microscopic observation (Zeiss), the skull was incised in the middle, the bulla was removed, and the cochlea was exposed. The cochlea was removed, placed in a glass dish containing 4% paraformaldehyde in PBS, and perfused with the incubation solution *via* a small hole in the apex and openings in the round and oval windows at the base. After incubation in 8% EDTA in phosphate buffer at room temperature for 4–5 h, the stria vascularis, vestibular membrane and tectorial membrane were carefully separated, and the sensory epithelium was dissected out. The auditory hair cells in the middle part of the cochlea are used to study immunofluorescence staining.

### Immunofluorescence staining and laser scanning confocal microscopic imaging

The separated basilar membrane was incubated in 0.5% Triton X-100 for 20 min, washed with PBS (3 times, 5 min each time), and blocked in 5% normal donkey serum at room temperature for 2 h. An mouse anti-adaptin  $\alpha$  antibody (BD biosciences, 1:50) was then added, and the sample was incubated overnight in a 4°C refrigerator (>10 h). It was then removed, washed with PBS (3 times, 5 min each time),

incubated with donkey anti-mouse IgG (1:500) at room temperature (25°C) in the dark for 45 min, washed with PBS (3 times, 5 min each time), incubated with DAPI (Sigma) for 10 min, and rinsed with PBS. Finally, the basilar membrane was laid flat on a microslide, and two drops of anti-fluorescent quench sealant were added. The location of the AP-2 protein in the HCs was then observed. Labeling of myosin VI (Santa Cruz, 1:50) and DAPI labeling were performed separately. The samples were examined by laser confocal microscopy (Zeiss) using a 60x oil-immersion objective for observation and photography at excitation wavelengths of 488 nm (FITC) and 594 nm (Alexa). The IHCs in the observed area were scanned from top to bottom, and images of each layer were observed continuously.

### Software analysis of AP-2 and myosin VI protein immunofluorescence intensity

ZEN lite 2020 software (ZEISS) was used to quantitatively analyze the expression of AP-2 and myosin VI by measuring the immunofluorescence intensity mean value (IMV). Five IHCs were selected from each group of animals, and 10 regions of equal area were analyzed for IMV measurement. Previous studies have shown that active endocytosis occurs at or near the basolateral area of IHCs. IHCs play a key role in hearing development and maintenance [19]. We measured the immunofluorescence IMV of the selected areas near the basolateral areas of the IHCs and obtained a total of 40 data points from four groups for statistical analysis (T-test).

### Real-time fluorescence quantification PCR (qRT-PCR)

The organ of Corti was dissected, isolated and quickly ground in RNAiso Plus solution. Its total RNA was extracted using the Trizol method, and the concentration and purity of the isolated RNA were determined by spectrophotometry. Total RNA was reverse-transcribed into cDNA using a reverse transcription kit according to the manufacturer's instructions and stored at -20°C. The primers used in reverse transcription were designed and produced by Shanghai Biotech Software. The upstream and downstream primers were AP2a2: CAATCCACAGCAAGAAGTGC (forward) and GCAACAAGCAGCCAATCTG (reverse); myosin VI: AGTCGTAAGTGCGCTGAAAGA (forward) and TGTATCTGCTCCCTCGTCATC (reverse).  $\beta$ -actin was used as an internal reference. The sample was pre-denatured at 95°C for 10 min and then subjected to 40 cycles of 95°C for 15 s, 60°C for 30 s, 72°C for 50 s, and 72°C for 5 s. The obtained experimental data were analyzed to obtain the Ct value of the mRNA. The comparison of expression levels was based on the Livak method [20,21], which was used to calculate the relative quantity (RQ) value according to the following equation:  $RQ = 2^{-\Delta\Delta Ct}$ , where  $\Delta Ct$  = target gene average Ct value - internal reference gene base for average Ct value and  $\Delta\Delta Ct$  = experimental  $\Delta Ct$  - control group  $\Delta Ct$ . Using the mRNA expression level of P7 mice as a control, we compared the differences in RQ values between the experimental specimens and the control group.

### Statistical analysis

All data are presented as mean  $\pm$  SD. Statistical analysis of the experimental data was conducted using the one-way ANOVA Student–Newman–Keuls test, which is appropriate for determining significant differences between groups. A value of  $p < 0.05$  was considered statistically significant.

## Results

### Cellular localization of AP-2 and myosin VI in adult (8-week-old) CBA/CaJ mice

We used immunofluorescence to detect the localization and expression of AP-2 in mice. We found that AP-2 (Figure 1(A–C)) was mainly localized in the cytoplasmic region of IHCs and that it was expressed in the area where the ribbon synapse approached the afferent neurons. Myosin VI (Figure 1(D–F)) was highly expressed in the cytoplasm of IHCs and OHCs.

### Changes in ABR threshold with aging

To characterize the relationship among AP-2, myosin VI and aging, we first measured the ABR threshold of mice of different ages. As shown in Figure 2, there was no significant difference between the P15 group and the P35 group in ABR threshold. However, we found that the ABR threshold

of 16-month-old mice increased significantly ( $p < 0.05$ ), indicating the occurrence of hearing damage.

### Expression of AP-2 and myosin VI in HCs of mice of different ages

To characterize possible changes in the expression patterns of AP-2 and myosin VI with aging, we used immunofluorescence to label these two proteins in the cochleae of mice of different ages. We found that the expression of AP-2 and myosin VI varied with age. The fluorescence intensity of both AP-2 (Figure 3(A'–C')) and myosin VI (Figure 4(E'–G')) increased significantly from P7 to P35 ( $p < .05$ ). The expression of AP-2 (Figure 3(C'–D')) and myosin VI (Figure 4(G'–H')) was highest in the P35 group, and it decreased significantly in the 16-month-old group ( $p < .05$ ). The results are shown in Figure 5. The expression of AP-2 and myosin VI was significantly increased in both the P15 group and the P35 group ( $p < .05$ ) compared with the P7 group, and it was decreased in the 16-month-old group compared with the P35 group.

### Comparison of AP-2 and myosin VI mRNA levels in HCs of different groups of mice by RT-qPCR

We used PCR to verify the differential expression of AP-2 and myosin VI. As shown in Figure 6, the mRNA expression

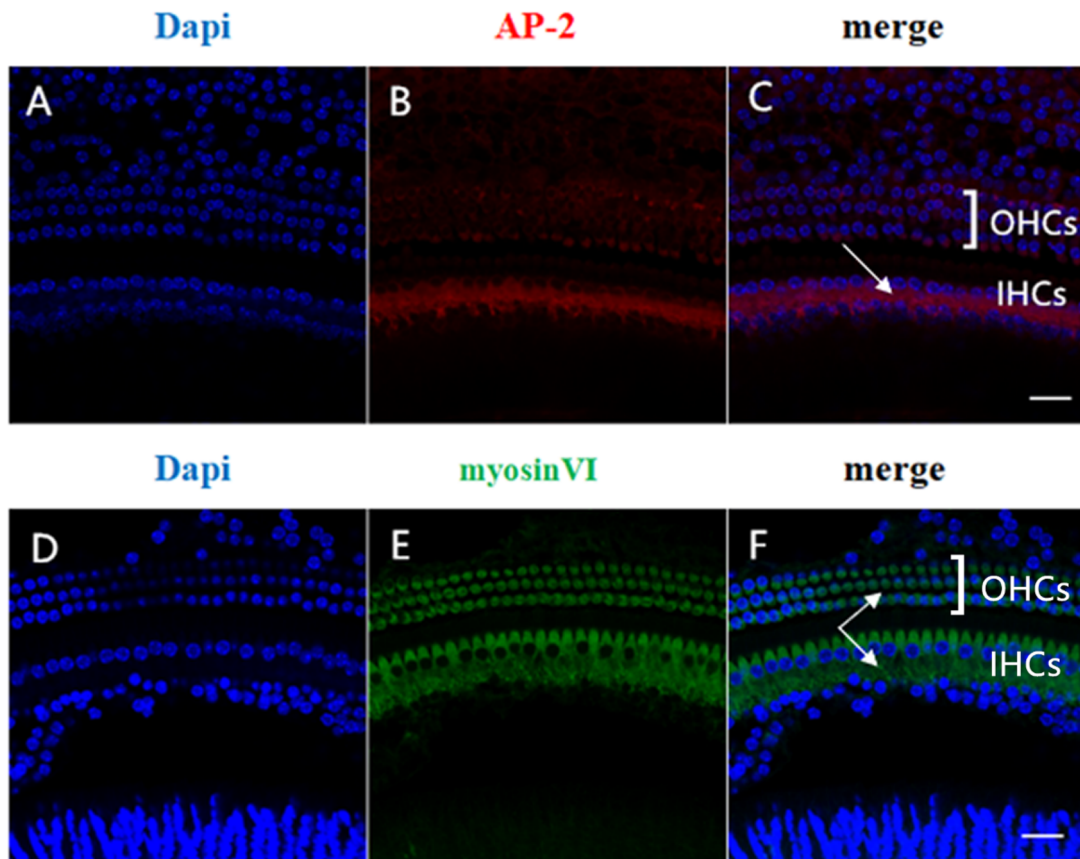


**Figure 1.** Localization and expression of AP-2 and myosin VI in adult mouse cochlea. Panels A–C show AP-2 labeling (red) and DAPI staining (blue). AP-2 (B) was highly expressed in IHCs but not in OHCs and intensely expressed in the synaptic regions of IHCs (C). D–F shows the dual labeling of myosin VI (green) and DAPI staining (blue). myosin VI (E) was highly expressed in both IHCs and OHCs, mainly in the cytoplasmic regions of the cells. Scale bar = 20  $\mu$ m.

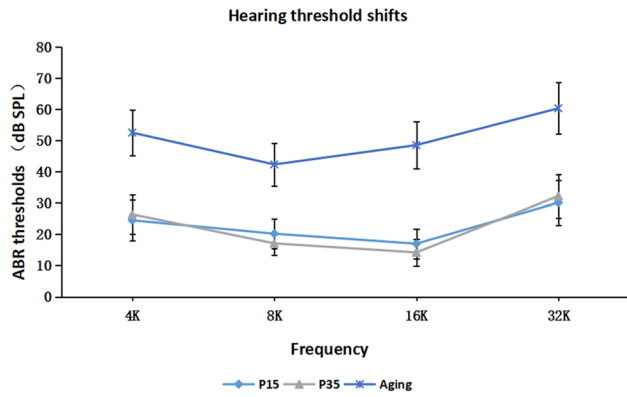


**Figure 2.** ABR thresholds in mice of different ages. ABR thresholds were recorded in P7, P15, P35 and 16-month-old (aging) mice ( $n=10$  in each group). The 16-month-old group showed a significant increase in ABR threshold compared with the P15 and P35 groups. The wave pattern observed at P7 was not stable and was not included in the analysis.

levels of AP-2 and myosin VI were lower in the P7 group than in the P15 and P35 groups ( $p<.05$ ). However, no significant difference was found between the P35 group and the 16-month-old group ( $p>.05$ ).

## Discussions

Recent studies of cochlear IHC ribbon synapses mainly focus on ribbon synapse morphology, number and vesicle exocytosis [6,22]. There are few reports on the physiology of endocytosis in cochlear HCs. The CME pathway is the main mechanism of vesicle recovery at ribbon synapses [23]. Otoferlin has been postulated to act as a calcium sensor for exocytosis as well as to be involved in rapid vesicle replenishment in IHCs [24], and otoferlin-AP-2 interaction drives  $\text{Ca}^{2+}$ - and stimulus-dependent compensating CME in mature IHCs. AP-2 might involve the C2-domain of otoferlin, may enhance the lateral diffusion of otoferlin and associated vesicular proteolipid [25,26]. AP-2 is the core protein of clathrin-coated vesicles (CCVs) and plays a significant role in the receptor-mediated endocytic recovery of synaptic vesicles [27,28]. It is a heterotetramer consisting of four subunits ( $\alpha$ ,  $\beta 2$ ,  $\mu 2$ , and  $\sigma 2$ ). AP-2 recognizes vesicle components and combines with other endocytic proteins to initiate the endocytosis process [29]. Myosin VI is the only protein in the myosin family that moves toward the negative terminal of the microfilament. Myosin VI promotes the movement of vesicles to the cytosol. AP-2 and myosin VI are known as proteins that play key roles in regulating the structure and dynamics of CME. After the formation of vesicles in the middle and late stages of endocytosis, AP-2/myosin VI-mediated vesicles are transported from the plasma membrane to the intracellular, causing the neck of the vesicle to become narrower. Finally, vesicles are shear-separated from the plasma membrane [14].

We first determined the location and expression of AP-2 and myosin VI. We found that AP-2 was localized in the cytosol of cochlear IHCs and mainly expressed at the base of IHCs, especially in the area where IHC ribbon synapses

contact the afferent neurons. Myosin VI protein was expressed in the cytoplasm of IHCs and OHCs. The ribbon synapse is the initial structure of the auditory nerve pathway and is characterized by its rapid and sustainable release of vesicles. AP-2/myosin VI is crucial for the internalization of vesicles after their detachment from the plasma membrane. Regulation of the compound might affect vesicle endocytosis and result in altered synaptic function.

In the central nervous system, AP-2 protein is mainly expressed in the cytoplasm and dendrites of hippocampal neurons [30]. Research has shown that the AMPA receptor cytoplasmic tail region recognizes synaptotagmin 1 by combining with the  $\mu$  subunit of the AP-2 protein, thereby mediating the internalization of ionotropic glutamate receptors and increasing the number of glutamate receptors [31,32]. The AP-2 protein is involved in the pathogenesis of central nervous system diseases such as Alzheimer's disease, ischemia-reperfusion injury, Huntington's disease, epileptic encephalopathies (DEEs) and others [33,34]. Myosin VI mainly contributes to anchoring and transport. Its gene, MYO6, is associated with DFNA22-type and DFNB37-type hereditary hearing impairment in humans [34]. Mutant mice (Snell's Waltzer mice) exhibit hearing and vestibular dysfunction [35]. It is widely accepted that glutamate is the main neurotransmitter released at cochlear IHC synapses and that it is related to diseases such as noise, age-related hearing impairment and acoustic neuropathy [36,37]. This glutamate, which is closely associated with excitatory toxicity at IHC ribbon synapses, can lead to edema of afferent nerve dendrites, resulting in hearing impairment. Research has shown that Dab2 can recruit myosin VI and bind to the end of the myosin VI molecule through specific sites so as to mediate the association of the myosin VI molecule with AP-2 [38]. Moreover, the AP-2/myosin VI complex is a key structural and functional protein complex that mediates glutamate neurotransmitter endocytosis, and changes in its expression are of great significance in the study of nerve-related deafness.

Based on research on auditory development maturation in mice [15], we have selected four age groups: 7 days post-birth (representing a cochlear structure that is essentially perfect), 15 days (exhibiting stable ABR, CAP latency and amplitude, as well as mature electrical activity of the cochlea), 35 days (entering a slower growth period across various developmental stages, essentially reaching physical maturity), and 16 months (old age).

The selection of P7 mice, which are in the neonatal period when the auditory system is at its primary stage of development, facilitates the investigation of early developmental processes within the auditory system. By measuring the ABR thresholds of mice at different stages of growth and development, it was found that the ABR response of the mice in the P7 group was not stable. This might be due to the fact that P7 mice still have closed ear canals or be related to the immaturity of IHCs, which cannot maintain a stable, sustained and rapid  $\text{Ca}^{2+}$  current and fail to generate spontaneous or evoked action potentials, ultimately affecting the continuous release of synaptic vesicles. The auditory function of P15 mice has reached a stable state, rendering

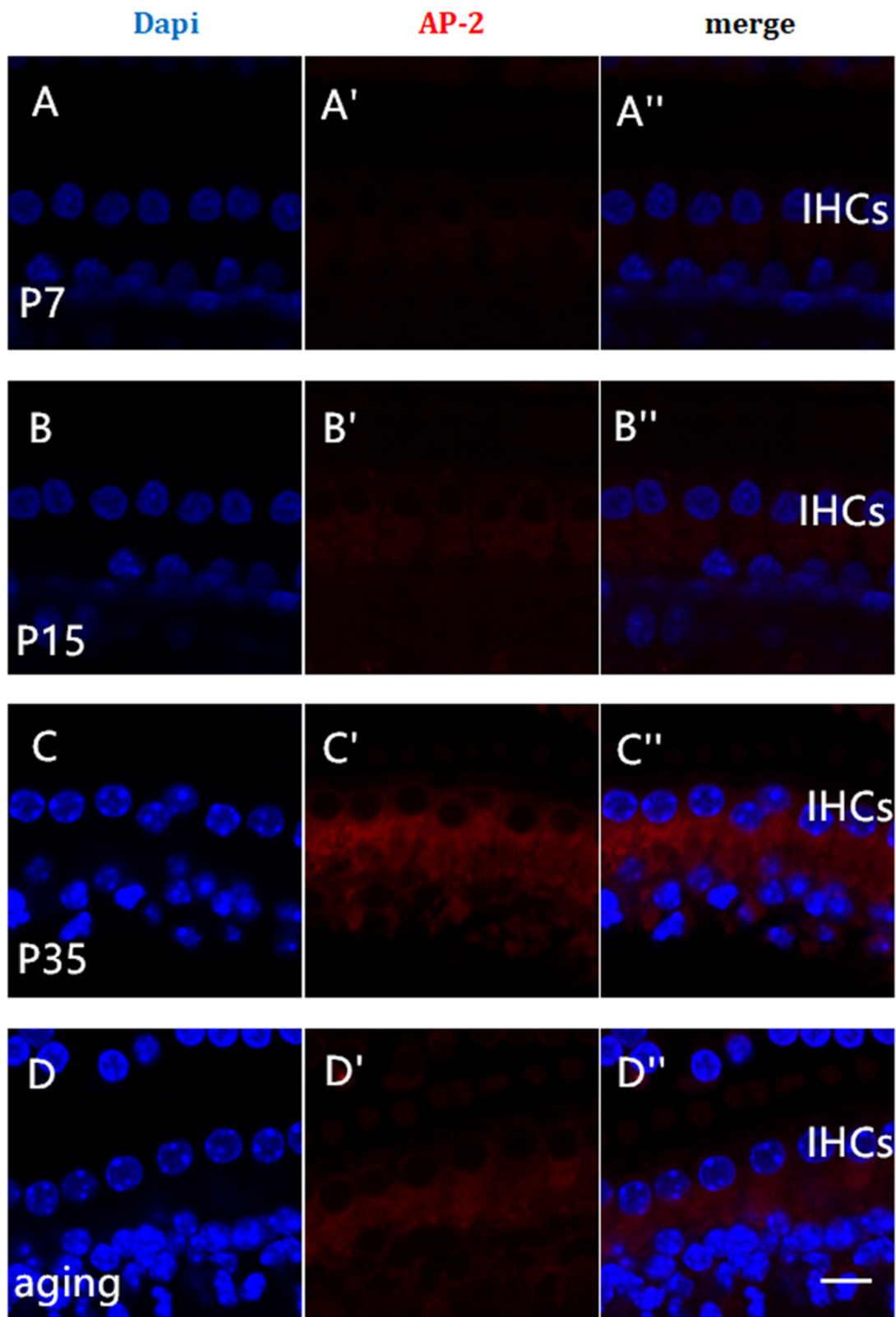


**Figure 3.** Expression of AP-2 protein in the cochleae of mice of different ages. The tissue was immunohistochemically stained for AP-2 (red) and examined by confocal microscopy. Nuclei were labeled with DAPI (blue). Postnatal day 7 (P7), A–A''; P15, B–B''; P35, C–C''; 16-month-old (aging), D–D''. Panels A''–D'' show the merged images. Scale bar = 5  $\mu$ m.

them suitable for investigating the normal functioning of the auditory system. Selecting mice during this period facilitates the study of hearing function in its mature state. Compared with mice in the P7 and P15 groups, the IMV of AP-2 and

myosin VI and mRNA expression is significantly increased ( $p < 0.05$ ), indicating that AP-2 and myosin VI proteins may play important roles in the development of auditory function. This might be related to the fact that at this age, IHC

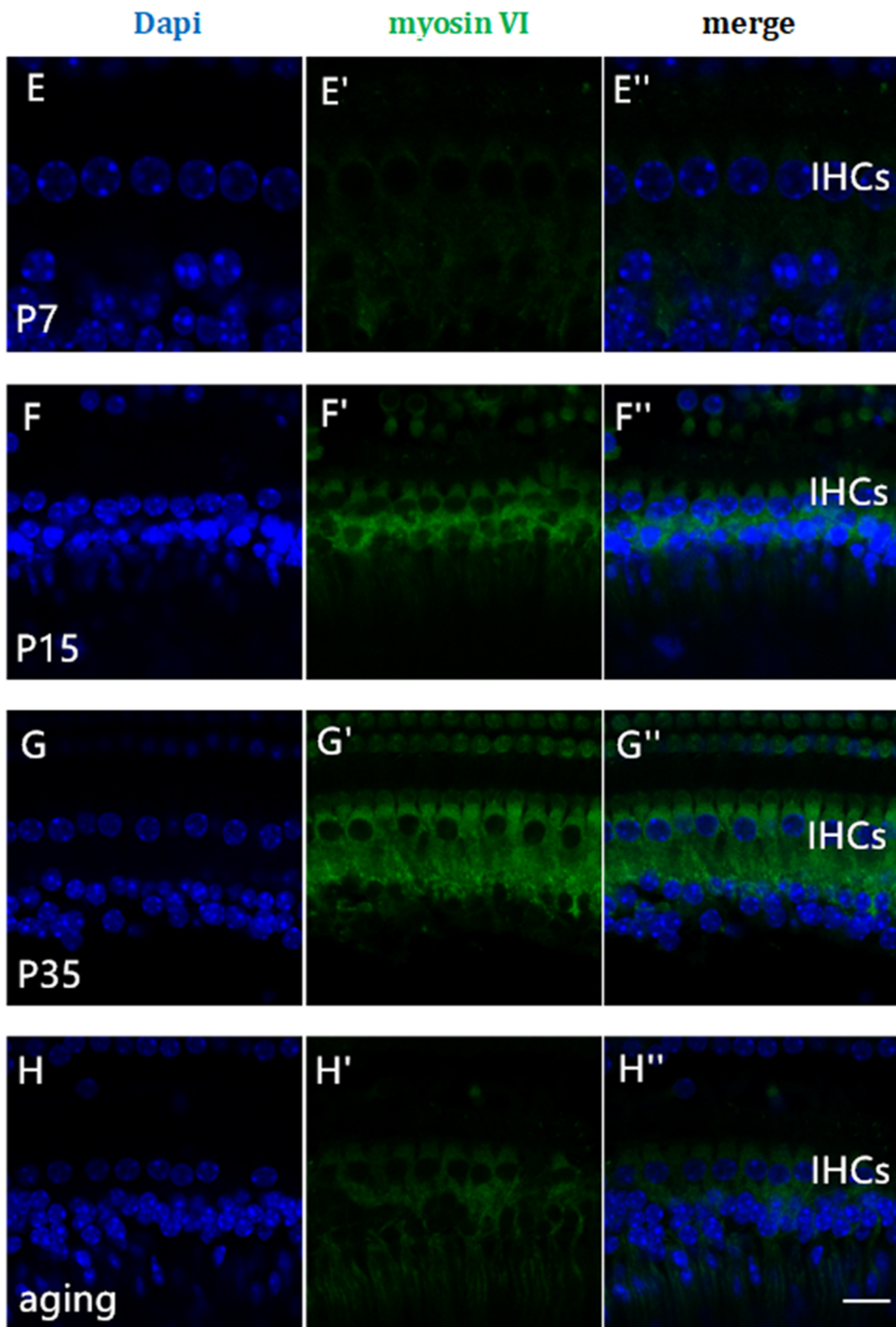


**Figure 4.** Variations in myosin VI protein expression in the cochleae of mice of different ages. The tissue was immunohistochemically stained for myosin VI (green) and examined by confocal microscopy. Nuclei were visualized with DAPI (blue). Postnatal day 7 (P7), E–E''; P15, F–F''; P35, G–G''; 16-month-old (aging), H–H''. Panels E''–H'' show the merged images. Scale bar = 5  $\mu$ m.

ribbon synapses are undergoing continuous development and elaborate synaptic connections are forming. The ABR threshold of the mice in the P7 group was not stable; the reason for this might be that AP-2 and myosin VI were

underexpressed, and the CME pathways they normally regulate were therefore unable to mediate the continuous endocytosis of vesicles. After the immature IHCs released synaptic vesicles in response to a slow  $\text{Ca}^{2+}$  current, the released

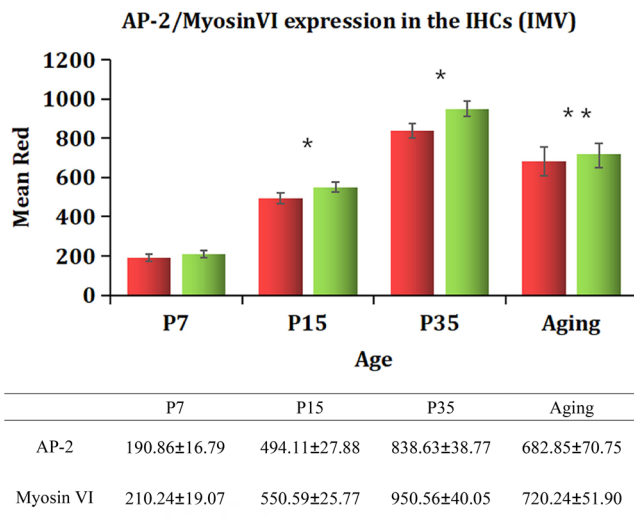


**Figure 5.** Variations in AP-2 and myosin VI immunofluorescence IMV in the cochleae of mice of different ages. A densitometric analysis of AP-2 and myosin VI expression in the IHCs of mice of different ages was performed. Regions of equal area ( $9\mu\text{m}^2$ ) were selected for IMV measurement, and the results were analyzed by ANOVA. The data are expressed as the mean±standard deviation of the values obtained in at least three independent experiments. The error bars represent standard deviation. AP-2 (red), myosin VI (green). \* $p<.05$  vs. P7; \*\* $p<.05$  vs. P35.

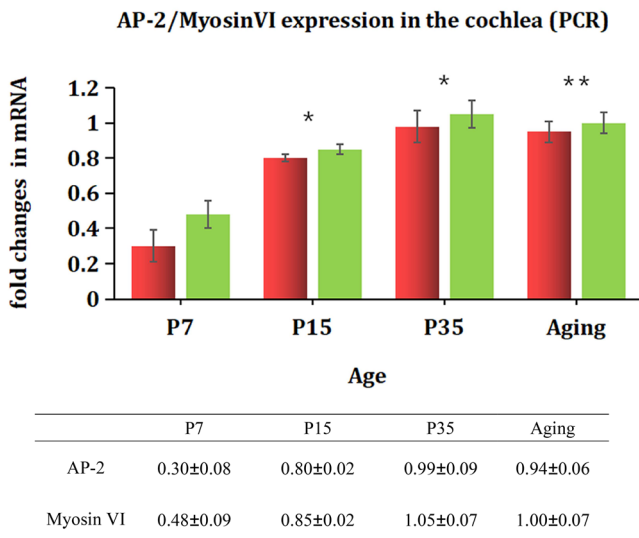


**Figure 6.** Variations in the expression of myosin VI and AP2 mRNAs in the cochleae of mice of different ages. The mRNA expression of AP-2 and myosin VI in the cochleae of mice was examined by quantitative real-time qRT-PCR. AP-2 (red), myosin VI (green). \* $p<.05$  vs. P7; \*\* $p>.05$  vs. P35.

vesicles could not be effectively recovered by endocytosis of the presynaptic membrane, and this affected the vesicle circulation. Between 7 and 35 days of postnatal development, along with the development of the inner ear, the endocytic recovery function of the vesicles was gradually completed.

ARHL is caused by multiple mechanisms and multiple pathways, and its underlying mechanisms may be related to factors such as central auditory degradation, lipid peroxidation damage, apoptosis and excitatory neurotoxicity [39,40]. The P35 mice exhibit a physiological equivalence to middle-aged humans, with the maturation of various organ

systems such as the digestive, circulatory, and nervous systems. This enables them to more accurately replicate the physiological responses and disease processes observed in adult animals. At 16 months old, mice reach a senile stage comparable to that of humans, making them an ideal model for investigating senile diseases. Compared with the elderly group, the immunofluorescence IMVs of AP-2 and myosin VI were significantly increased in the P35 group ( $p<.05$ ). However, PCR analysis of the expression levels of the mRNAs encoding the target proteins showed no statistically significant difference ( $p>.05$ ). This might be due to imbalances in the levels of transcription and post-translational proteins in senile mice. The number of AP-2 and myosin VI proteins in senile mice might not decrease significantly. A lack of sufficient amounts of functional AP-2 and myosin VI proteins to regulate the pathway of CME could lead to excessive accumulation of glutamate at the afferent synapses. Glutamate causes nerve excitotoxicity that can cause edema of afferent nerve dendrites and lead to the eventual occurrence of hearing damage. qRT-PCR essentially detects the amount of mRNA produced by gene transcription. The finding that the mRNA levels of these proteins were higher in the P35 group may be related to changes in mRNA modification and translation or to changes in protein degradation in aging mice compared with adult mice. In general, it was found that the expression of the two proteins first increased and then decreased after birth. The conformation and function of the AP-2/myosin VI itself may also affect IHC function. The ABR threshold of the elderly group was higher than that of the P35 group, but how the levels of the studied proteins, IHC function and the animals' hearing function are related should be further explored in combination with functional experiments. During the process of auditory maturation and aging, changes in the functions of IHCs can occur, and these changes are probably associated with AP-2/myosin VI.

The influence of a specific protein on age-related changes in hearing function is indeed a topic worthy of thorough exploration. The growth and subsequent decline of this protein after birth may involve intricate mechanisms at multiple levels. Firstly, at the transcriptional level, various factors associated with aging including genetic factors, environmental factors, and physiological aging can influence gene expression of this protein leading to alterations in gene transcription activity which subsequently affects its synthesis. In elderly mice, reduced transcriptional activity could potentially impact hearing function by decreasing protein synthesis. Secondly, post-translational modification plays a crucial role as the synthesized protein undergoes several processes such as glycosylation and phosphorylation that affect its stability and functionality. With advancing age, these processes may change leading to damage or loss of protein function. Additionally, excessive degradation due to age could result in decreased levels of the protein. An imbalance between transcription and post-translational modifications is possible due to physiological aging and other factors which negatively impact gene transcription and ultimately cause reduced expression levels that directly affect auditory system-related proteins functionality thereby influencing hearing function.

The developmental maturation of the peripheral auditory pathway is a highly complex process, and the onset of hearing does not depend on synaptic function alone but also on various other factors, including the morphological and functional maturation of hair bundle mechanotransduction, OHC electromotility, and the IHC exocytosis machinery. The experiments performed in this study measured the expression of AP-2 and myosin VI in cochlear HCs. By analyzing differences in the hearing function of mice at different stages of growth and development, we preliminarily found that the expression patterns of AP-2 and myosin VI in the mouse cochlea are consistent with the development of the auditory system. The expression levels of these proteins may change at different ages, and this probably leads to differences in the efficiency of CME; it may also cause a defect in IHC function. It is of great significance to study the dynamic regulation of vesicle internalization. Based on previous literature [38] and bioinformatics screening, we also found that Dab2 is the protein most likely to be the signal molecule that regulates the formation of the AP-2/myosin VI complex, thereby affecting vesicle internalization. Our subsequent investigation aims to elucidate the involvement of Dab2 in the regulation of AP-2/Myosin VI complex thereby influencing hair cell vesicle internalization process. Through this study, the proteins that participate in the signaling pathway leading to the internalization of synaptic vesicle recovery in cochlear IHCs were clarified, and the possible cause of sensorineural hearing loss was explained from the perspective of vesicle recovery through endocytosis. It is hoped that this work will provide a theoretical basis for the prevention of auditory impairment.

## Disclosure statement

No potential conflict of interest was reported by the author(s).

## Funding

This study was funded by Wuhan Health Commission Fund: WX21Q51

## References

- [1] Michanski S, Kapoor R, Steyer AM, et al. Piccolino is required for ribbon architecture at cochlear inner hair cell synapses and for hearing. *EMBO Rep.* 2023;24(9):e56702. doi: [10.15252/embr.202256702](https://doi.org/10.15252/embr.202256702).
- [2] Lu Y, Liu J, Li B, et al. Spatial patterns of noise-induced inner hair cell ribbon loss in the mouse mid-cochlea. *iScience.* 2024;27(2):108825. doi: [10.1016/j.isci.2024.108825](https://doi.org/10.1016/j.isci.2024.108825).
- [3] Tan WJT, Vlajkovic SM. Molecular characteristics of cisplatin-induced ototoxicity and therapeutic interventions. *Int J Mol Sci.* 2023;24(22):16545. doi: [10.3390/ijms242216545](https://doi.org/10.3390/ijms242216545).
- [4] Okur MN, Sahbaz BD, Kimura R, et al. Long-term NAD<sup>+</sup> supplementation prevents the progression of age-related hearing loss in mice. *Aging Cell.* 2023;22(9):e13909. doi: [10.1111/acel.13909](https://doi.org/10.1111/acel.13909).
- [5] Calvet C, Peineau T, Benamer N, et al. The SNARE protein SNAP-25 is required for normal exocytosis at auditory hair cell ribbon synapses. *iScience.* 2022;25(12):105628. doi: [10.1016/j.isci.2022.105628](https://doi.org/10.1016/j.isci.2022.105628).
- [6] Kurasawa S, Mohri H, Tabuchi K, et al. Loss of synaptic ribbons is an early cause in ROS-induced acquired sensorineural hearing loss. *Neurobiol Dis.* 2023;186:106280. doi: [10.1016/j.nbd.2023.106280](https://doi.org/10.1016/j.nbd.2023.106280).
- [7] Milosevic I. Revisiting the role of clathrin-mediated endocytosis in synaptic vesicle recycling. *Front Cell Neurosci.* 2018;12:27. doi: [10.3389/fncel.2018.00027](https://doi.org/10.3389/fncel.2018.00027).
- [8] Maritzen T, Haucke V. Coupling of exocytosis and endocytosis at the presynaptic active zone. *Neurosci Res.* 2018;127:45–52. doi: [10.1016/j.neures.2017.09.013](https://doi.org/10.1016/j.neures.2017.09.013).
- [9] Kaksonen M, Roux A. Mechanisms of clathrin-mediated endocytosis. *Nat Rev Mol Cell Biol.* 2018;19(5):313–326. doi: [10.1038/nrm.2017.132](https://doi.org/10.1038/nrm.2017.132).
- [10] Partlow EA, Cannon KS, Hollopeter G, et al. Structural basis of an endocytic checkpoint that primes the AP2 clathrin adaptor for cargo internalization. *Nat Struct Mol Biol.* 2022;29(4):339–347. doi: [10.1038/s41594-022-00749-z](https://doi.org/10.1038/s41594-022-00749-z).
- [11] Ramesh ST, Navyasree KV, Sah S, et al. BMP2K phosphorylates AP-2 and regulates clathrin-mediated endocytosis. *Traffic.* 2021;22(11):377–396. doi: [10.1111/tra.12814](https://doi.org/10.1111/tra.12814).
- [12] Biancospino M, Buel GR, Niño CA, et al. Clathrin light chain a drives selective myosin VI recruitment to clathrin-coated pits under membrane tension. *Nat Commun.* 2019;10(1):4974. doi: [10.1038/s41467-019-12855-6](https://doi.org/10.1038/s41467-019-12855-6).
- [13] Wagner W, Lippmann K, Heisler FF, et al. Myosin VI drives clathrin-mediated AMPA receptor endocytosis to facilitate cerebellar long-term depression. *Cell Rep.* 2019;28(1):11–20.e9. doi: [10.1016/j.celrep.2019.06.005](https://doi.org/10.1016/j.celrep.2019.06.005).
- [14] Tumbarello DA, Kendrick-Jones J, Buss F. Myosin VI and its cargo adaptors - linking endocytosis and autophagy. *J Cell Sci.* 2013;126(Pt 12):2561–2570. doi: [10.1242/jcs.095554](https://doi.org/10.1242/jcs.095554).
- [15] Bulankina AV, Moser T. Neural circuit development in the mammalian cochlea. *Physiology (Bethesda).* 2012;27(2):100–112. doi: [10.1152/physiol.00036.2011](https://doi.org/10.1152/physiol.00036.2011).
- [16] Chang A, Chen P, Guo S, et al. Specific influences of early acoustic environments on cochlear hair cells in postnatal mice. *Neural Plast.* 2018;2018:5616930–5616913. doi: [10.1155/2018/5616930](https://doi.org/10.1155/2018/5616930).
- [17] Xiong W, Wei W, Qi Y, et al. Autophagy is required for remodeling in postnatal developing ribbon synapses of cochlear inner hair cells. *Neuroscience.* 2020;431:1–16. doi: [10.1016/j.neuroscience.2020.01.032](https://doi.org/10.1016/j.neuroscience.2020.01.032).
- [18] Vincent PFY, Young ED, Edge ASB, et al. Auditory hair cells and spiral ganglion neurons regenerate synapses with refined release properties in vitro. *bioRxiv.* 2023; Dec 2:2023.10.05.561095. doi: [10.1101/2023.10.05.561095](https://doi.org/10.1101/2023.10.05.561095).
- [19] Li S, Yu S, Ding T, et al. Different patterns of endocytosis in cochlear inner and outer hair cells of mice. *Physiol Res.* 2019;68(4):659–665. doi: [10.33549/physiolres.934009](https://doi.org/10.33549/physiolres.934009).
- [20] Livak KJ, Schmittgen TD. Analysis of relative gene expression data using real-time quantitative PCR and the 2(-Delta Delta C(T)) method. *Methods.* 2001;25(4):402–408. doi: [10.1006/meth.2001.1262](https://doi.org/10.1006/meth.2001.1262).
- [21] Ballester M, Cerdón R, Folch JM. DAG expression: high-throughput gene expression analysis of real-time PCR data using standard curves for relative quantification. *PLoS One.* 2013;8(11):e80385. doi: [10.1371/journal.pone.0080385](https://doi.org/10.1371/journal.pone.0080385).
- [22] Chen H, Fang Q, Benseler F, et al. Probing the role of the C(2) F domain of otoferlin. *Front Mol Neurosci.* 2023;16:1299509. doi: [10.3389/fnmol.2023.1299509](https://doi.org/10.3389/fnmol.2023.1299509).
- [23] Neef J, Jung S, Wong AB, et al. Modes and regulation of endocytic membrane retrieval in mouse auditory hair cells. *J Neurosci.* 2014;34(3):705–716. doi: [10.1523/JNEUROSCI.3313-13.2014](https://doi.org/10.1523/JNEUROSCI.3313-13.2014).
- [24] Ford CL, Riggs WJ, Quigley T, et al. The natural history, clinical outcomes, and genotype-phenotype relationship of otoferlin-related hearing loss: a systematic, quantitative literature review. *Hum Genet.* 2023;142(10):1429–1449. doi: [10.1007/s00439-023-02595-5](https://doi.org/10.1007/s00439-023-02595-5).
- [25] Duncker SV, Franz C, Kuhn S, et al. Otoferlin couples to clathrin-mediated endocytosis in mature cochlear inner hair cells. *J Neurosci.* 2013;33(22):9508–9519. doi: [10.1523/JNEUROSCI.5689-12.2013](https://doi.org/10.1523/JNEUROSCI.5689-12.2013).

- [26] Jung S, Maritzen T, Wichmann C, et al. Disruption of adaptor protein 2mu (AP-2mu) in cochlear hair cells impairs vesicle re-loading of synaptic release sites and hearing. *Embo J.* 2015;34(21): 2686–2702. doi: [10.15252/embj.201591885](https://doi.org/10.15252/embj.201591885).
- [27] Ritter B, Murphy S, Dokainish H, et al. NECAP 1 regulates AP-2 interactions to control vesicle size, number, and cargo during clathrin-mediated endocytosis. *PLoS Biol.* 2013;11(10):e1001670. doi: [10.1371/journal.pbio.1001670](https://doi.org/10.1371/journal.pbio.1001670).
- [28] Boucrot E, Saffarian S, Zhang R, et al. Roles of AP-2 in clathrin-mediated endocytosis. *PLoS One.* 2010;5(5):e10597. doi: [10.1371/journal.pone.0010597](https://doi.org/10.1371/journal.pone.0010597).
- [29] Yap CC, Winckler B. Adapting for endocytosis: roles for endocytic sorting adaptors in directing neural development. *Front Cell Neurosci.* 2015;9:119. doi: [10.3389/fncel.2015.00119](https://doi.org/10.3389/fncel.2015.00119).
- [30] Kastning K, Kukhtina V, Kittler JT, et al. Molecular determinants for the interaction between AMPA receptors and the clathrin adaptor complex AP-2. *Proc Natl Acad Sci U S A.* 2007;104(8): 2991–2996. doi: [10.1073/pnas.0611170104](https://doi.org/10.1073/pnas.0611170104).
- [31] Ahmadian G, Ju W, Liu L, et al. Tyrosine phosphorylation of GluR2 is required for insulin-stimulated AMPA receptor endocytosis and LTD. *Embo J.* 2004;23(5):1040–1050. doi: [10.1038/sj.emboj.7600126](https://doi.org/10.1038/sj.emboj.7600126).
- [32] DaSilva LLP, Wall MJ, P de Almeida L, et al. Activity-regulated cytoskeleton-associated protein controls AMPAR endocytosis through a direct interaction with clathrin-adaptor protein 2. *eNeuro.* 2016;3(3):ENEURO.0144-15.2016. doi: [10.1523/ENEURO.0144-15.2016](https://doi.org/10.1523/ENEURO.0144-15.2016).
- [33] Helbig I, Lopez-Hernandez T, Shor O, et al. A recurrent missense variant in AP2M1 impairs Clathrin-Mediated endocytosis and causes developmental and epileptic encephalopathy. *Am J Hum Genet.* 2019;104(6):1060–1072. doi: [10.1016/j.ajhg.2019.04.001](https://doi.org/10.1016/j.ajhg.2019.04.001).
- [34] Katsumata Y, Fardo DW, Bachstetter AD, et al. Alzheimer disease pathology-associated polymorphism in a complex variable number of tandem repeat region within the MUC6 gene, near the AP2A2 gene. *J Neuropathol Exp Neurol.* 2020;79(1):3–21. doi: [10.1093/jnen/nlz116](https://doi.org/10.1093/jnen/nlz116).
- [35] Hegan PS, Kravtsov DV, Caputo C, et al. Restoration of cytoskeletal and membrane tethering defects but not defects in membrane trafficking in the intestinal brush border of mice lacking both myosin Ia and myosin VI. *Cytoskeleton (Hoboken).* 2015; 72(9):455–476. doi: [10.1002/cm.21238](https://doi.org/10.1002/cm.21238).
- [36] Liu H, Lu J, Wang Z, et al. Functional alteration of ribbon synapses in inner hair cells by noise exposure causing hidden hearing loss. *Neurosci Lett.* 2019;707:134268. doi: [10.1016/j.neulet.2019.05.022](https://doi.org/10.1016/j.neulet.2019.05.022).
- [37] Moser T, Starr A. Auditory neuropathy–neural and synaptic mechanisms. *Nat Rev Neurol.* 2016;12(3):135–149. doi: [10.1038/nrneurol.2016.10](https://doi.org/10.1038/nrneurol.2016.10).
- [38] Ungewickell EJ, Hinrichsen L. Endocytosis: clathrin-mediated membrane budding. *Curr Opin Cell Biol.* 2007;19(4):417–425. doi: [10.1016/j.ceb.2007.05.003](https://doi.org/10.1016/j.ceb.2007.05.003).
- [39] Yang J, Shao Z, Zhang D, et al. Pathogenesis and treatment progress in age-related hearing loss: a literature review. *Int J Clin Exp Pathol.* 2023;16(11):315–320.
- [40] Feng S, Yang L, Hui L, et al. Long-term exposure to low-intensity environmental noise aggravates age-related hearing loss via disruption of cochlear ribbon synapses. *Am J Transl Res.* 2020;12(7): 3674–3687.